

Seasonal Hydroclimate Variability over North America in Global and Regional Reanalyses and AMIP Simulations: Varied Representation

SUMANT NIGAM

Department of Atmospheric and Oceanic Science, and Earth System Science Interdisciplinary Center, University of Maryland, College Park, College Park, Maryland

ALFREDO RUIZ-BARRADAS

Department of Atmospheric and Oceanic Science, University of Maryland, College Park, College Park, Maryland

(Manuscript received 11 May 2005, in final form 8 August 2005)

ABSTRACT

The monotony of seasonal variability is often compensated by the complexity of its spatial structure—the case in North American hydroclimate. The structure of hydroclimate variability is analyzed to provide insights into the functioning of the climate system and climate models.

The consistency of hydroclimate representation in two global [40-yr ECMWF Re-Analysis (ERA-40) and NCEP] and one regional [North American Regional Reanalysis (NARR)] reanalysis is examined first, from analysis of precipitation, evaporation, surface air temperature (SAT), and moisture flux distributions. The intercomparisons benchmark the recently released NARR data and provide context for evaluation of the simulation potential of two state-of-the-art atmospheric models [NCAR's Community Atmospheric Model (CAM3.0) and NASA's Seasonal-to-Interannual Prediction Project (NSIPP) atmospheric model].

Intercomparisons paint a gloomy picture: great divergence in global reanalysis representations of precipitation, with the eastern United States being drier in ERA-40 and wetter in NCEP in the annual mean by up to a third in each case; model averages are like ERA-40. The annual means, in fact, mask even larger but offsetting seasonal departures.

Analysis of moisture transport shows winter fluxes to be more consistently represented. Summer flux convergence over the Gulf Coast and Great Plains, however, differs considerably between global and regional reanalyses. Flux distributions help in understanding the choice of rainy season, especially the winter one in the Pacific Northwest; stationary fluxes are key.

Land–ocean competition for convection is too intense in the models—so much so that the oceanic ITCZ in July is southward of its winter position in the both simulations! The overresponsiveness of land is also manifest in SAT; the winter-to-summer change over the Great Plains is 5–9 K larger than in observations, with implications for modeling of climate sensitivity.

The nature of atmospheric water balance over the Great Plains is probed, despite unbalanced moisture budgets in reanalyses and model simulations. The imbalance is smaller in NARR but still unacceptably large, resulting from excessive evaporation in spring and summer. Adjusting evaporation during precipitation assimilation could lead to a more balanced budget.

Global and regional reanalysis will remain of limited use for hydroclimate studies until they comply with the operative water and energy balance constraints.

1. Introduction

Precipitation is an influential hydroclimate field. Its distribution, especially the annually repeating component—the seasonal cycle—has shaped agricultural prac-

tices and water resource management across the planet. Hydroclimate is however more than just precipitation: it refers to the near-surface climate elements that impact societal sustenance—surface temperature, soil moisture, and streamflow, for example. Hydroclimate impacts appear prominently in the core questions driving global change science. A region of great interest is North America, where water resources are recharged in winter/spring and expended in summer (the growing season).

Corresponding author address: Dr. Sumant Nigam, 3419 Computer and Space Sciences Bldg., University of Maryland, College Park, College Park, MD 20742-2425.
E-mail: nigam@atmos.umd.edu

The seasonal rhythms forced by the annual march of the sun are predictable, but the evolution of precipitation in any given year seldom follows the climatological track. Departures from the seasonal cycle, or seasonal anomalies, are of great interest from the societal impact and climate prediction perspectives, and also because their origin remains intriguing. The cause of U.S. Midwest floods during the summer of 1993, for instance, is still being debated. The seasonal cycle, on the other hand, has no such allure, being devoid of the prediction challenge. Its monotony in time is however more than compensated by its spatial complexity, which begs an explanation. The regional-to-subcontinental-scale precipitation distribution often results from interactions of the atmosphere, land surface (and vegetation), and the adjoining oceans, which makes the precipitation seasonal cycle more complex than the seasonal insolation changes.¹ Analysis of seasonal hydroclimate variability can thus provide insights into the functioning of the climate system and climate simulation models.

Precipitation is a key link between the atmospheric water and energy cycles. It exerts a profound influence on regional hydroclimate, impacting soil and air temperatures, soil moisture and atmospheric humidity, surface/subsurface run-off and evaporation, streamflow and drought incidence, etc. Analysis of precipitation variability and its causes has however been stymied by the lack of regional-to-subcontinental-scale measurements of hydroclimate fields—principally, evaporation and soil moisture—and limited understanding of the cloud/convection processes. Evaporation measurements are sparse and generally confined to the subgrid-scale basins, such as U.S. Department of Agriculture (USDA) watersheds, the Oklahoma Mesonet, and the Illinois Water Survey field sites. The uncertainty in evaporation estimates has however not deterred investigation of atmospheric water cycle variability. The authors recently completed an analysis of the local and remote water sources—evaporation and moisture fluxes, respectively—of warm-season precipitation variability over the U.S. Great Plains (Ruiz-Barradas and Nigam 2005, hereafter RBN). Interannual variability was the focus of the study, in part, because the models were anticipated to be more scripted in generation of seasonal variability, since model tuning exercises often target the observed seasonal cycle.

Current interest in seasonal-cycle variability stems

from the challenge of understanding the complex spatiotemporal structure of precipitation variability. The authors' recent finding of an exaggerated role of evaporation in generation of interannual precipitation variability over the Great Plains in the National Aeronautics and Space Administration (NASA) and National Centers for Atmospheric Research (NCAR) atmospheric model simulations (RBN) is another motivation.² Interestingly, global atmospheric reanalyses produced by the National Centers for Environmental Prediction (NCEP) and the 40-yr European Centre for Medium-Range Weather Forecasts (ECMWF) Re-Analysis (ERA-40) also yield different roles for evaporation, further motivating the present analysis. Investigation of water balance, particularly, the role of evaporation and moisture transports in production of summertime rainfall over the Great Plains, in both reanalysis and simulation datasets should shed light on the models' behavior in the context of interannual variability, since models could, conceivably, carry forward aspects of their seasonal-cycle training into the interannual domain.

An important feature of this study is its description of seasonal hydroclimate variability from the recently released North American Regional Reanalysis dataset (NARR; Mesinger et al. 2004; Mitchell et al. 2004). Salient features of NARR include the direct, additional assimilation of precipitation and radiances, high spatial and temporal resolution, and the use of an improved land surface model (NOAH; Ek et al. 2003). The precipitation representation is very realistic in NARR, as shown later (cf. Fig. 2); that is, the assimilation strategy has been effective, especially, in the atmosphere where other fields are also better represented. A corresponding improvement in the representation of land surface variables is however not assured since the assimilation strategy directly (and somewhat arbitrarily) nudges only atmospheric variables (select ones), as discussed later in sections 5 and 6. Despite this caveat, the interaction of realistic precipitation with a comprehensive land surface model in NARR enhances prospects of obtaining improved description of hydroclimate variability.

The NARR hydroclimate is intercompared with extant analyses of gridded station observations, satellite derived/constrained estimates, global reanalysis repre-

¹ This is reminiscent of the eastern tropical Pacific climate, where the SST seasonal cycle is driven by ocean-atmosphere-land interactions, and not directly by the local insolation changes (Mitchell and Wallace 1992; Nigam and Chao 1996).

² The nearly 50-yr-long simulations were produced at these centers with specified (observed) boundary conditions (SST and sea ice), much as integrations for the Atmospheric Model Intercomparison Project (AMIP; Gates et al. 1999). The integrations may be overconstrained by prescription of SST in the extratropical basins.

sentations, and state-of-the-art atmospheric model simulations in this study, benchmarking NARR products in the process. Ascertaining the dominant balances—at least, the relative ordering of terms—if not the atmospheric water budget is also attempted with the NARR dataset.

The hydroclimate representation in NCEP reanalysis has been examined before but not in the manner of this analysis: Mo and Higgins (1996) intercompared annual-mean and/or zonal-mean distributions in NCEP and NASA/Data Assimilation Office (DAO) reanalyses over a 9-yr (1985–93) period. Higgins et al. (1997) did focus on the United States but with a short, ENSO-active period (1985–89) climatology. Trenberth and Guillemot (1998) examined the atmospheric moisture and hydrological cycles using a more stable climatology (1979–95), but their global plots offer limited view of the regional-to-subcontinental-scale features over North America. The present analysis of U.S. hydroclimate will thus provide new insights on the veracity of NCEP's representation—and, of course, of the more recently available ERA-40 and NARR representations.

Precipitation and surface temperature are, perhaps, the best and most extensively measured hydroclimate fields,³ in contrast with evaporation, soil moisture and runoff. The precipitation seasonal cycle is thus well characterized, particularly, over the United States, with key features being widely known, as is evident from perusal of geography atlases. Hsu and Wallace (1976) succinctly describe these features as follows: an area of winter maxima in the Pacific Northwest, a broad area of early summer maxima over the U.S. Great Plains and Great Lakes, an area of weak spring maxima over the southern states, and a region of weak seasonal variability over the middle and north Atlantic states. New data sources, including satellite-based estimates, and improved sampling and analysis in recent decades have refined this characterization. The resolution of climate models also increased in this period, but without commensurate gains in simulation of precipitation. A notable, common simulation deficiency is the spurious summertime maximum in regional rainfall over eastern United States (Boyle 1998). Since this region is devoid of complex orography and attendant resolution challenges, model physics has been implicated more than resolution in generation of this spurious feature.

Moisture fluxes are a key link between precipitation

and circulation. The fluxes are however not as reliably known as precipitation since they depend on upper-air humidity and winds, which are sampled less extensively than the surface quantities. Starr and Peixoto (1958) estimated fluxes from the irregularly spaced radiosonde data, in pioneering calculations conducted at the Massachusetts Institute of Technology (MIT). Moisture fluxes, like precipitation, exhibit substantial regional and seasonal variations over the United States, as noted in many studies beginning with the seminal analysis of Rasmusson (1967, 1968); the description has since been refined by Roads et al. (1994), Rasmusson and Mo (1996), and Ropelewski and Yarosh (1998), among others.

Observations of the entire column are not needed for computation of the vertically integrated fluxes because humidity drops off rapidly with height. Extensive temporal sampling is however necessary in some regions for accurate computation of the time-averaged fluxes, for example, the southern Great Plains where diurnal variability of the low-level jet is strong. Moisture fluxes are currently computed from retrospective analyses, which are a suitable blend of observations and short-range numerical weather forecasts; the forecasts are produced in a nonoperational environment using a fixed data assimilation system. In view of considerable influence of the weather prediction model and data assimilation strategy on the resulting analyses, moisture fluxes are obtained from two global and one regional reanalysis in this study. Multiple flux estimates provide a measure of the involved uncertainties and serve to define the tolerance for model assessments.

Evaporation is amongst the most poorly measured hydroclimate fields. It has been estimated—residually—from atmospheric water-balance considerations in many studies. Obtained estimates show that evaporation is larger than precipitation over the Great Plains in summer, while the opposite is true in winter (e.g., Roads et al. 1994). Evaporation is now, typically, diagnosed from land surface models (Huang et al. 1996; Dirmeyer and Tan 2001) driven by observed meteorology, especially, precipitation and temperature, and yield evaporation and runoff. Intercomparison of evaporation estimates in context of atmospheric water balance is an important component of this study.

Model assessments are a focus of the present analysis, while its hydroclimate accent is in keeping with the societal impact concerns of the ongoing Intergovernmental Panel for Climate Change (IPCC) assessments. Assessments reveal model strengths and weaknesses and provide a context for interpreting model predictions of regional climate variability and change. Dy-

³ Their measurements provide key points of reference for the atmosphere–land surface interaction schemes included in climate models.

namically (or thermodynamically) oriented assessments can also produce credible hypotheses for model deficiencies, but do not, typically, provide immediate recipes for improving the model's physics.

Datasets are described in section 2. Observed and simulated precipitation and surface air temperature are intercompared in section 3. Stationary and transient moisture fluxes (and their convergence) are displayed in section 4, which also discusses causes of the winter rainy season in the Pacific Northwest. Summertime evaporation is intercompared in section 5, while the atmospheric water cycle over the Great Plains is analyzed in section 6. Concluding remarks follow in section 7.

2. Datasets

The resolution and salient features of several datasets analyzed in this study can be found in the authors' earlier paper (RBN). Gridded precipitation observations over the United States and Mexico come from NCEP's Climate Prediction Center (CPC; hereafter, referred as the U.S.–Mexico station dataset; <http://www.cpc.ncep.noaa.gov/products/precip/realtime/retro.html>). The satellite and rain-gauge-based precipitation estimates [CPC Merged Analysis of Precipitation (CMAP-2); Xie and Arkin 1996] are also analyzed. The Xie–Arkin record is shorter but valuable in view of the spotty coverage of the station-based datasets.

The contribution of local and remote water sources in seasonal hydroclimate variability is investigated using observationally constrained evaporation estimates. In addition to those provided by global reanalyses (NCEP and ERA-40) and one regional reanalysis (NARR), evaporation estimates produced at the National Oceanic and Atmospheric Administration's (NOAA) CPC (Huang et al. 1996) and the Center for Ocean–Land–Atmosphere Studies (Dirmeyer and Tan 2001) are used in model assessments; monthly, gridded values are available for several recent decades at near-degree-scale resolution.

The surface air temperature (SAT) data come from the combined land and marine temperature archive at the University of East Anglia (UEA; HadCRUT2; Rayner et al. 2003; Jones and Moberg 2003; <http://www.cru.uea.ac.uk/cru/data/temperature/>). The data are available on a $5^\circ \times 5^\circ$ global grid, as anomalies with respect to the 1961–90 base period climatology; ocean grid points contain sea surface temperature (SST) rather than marine air temperature, for reasons stated in the above papers.

The nearly 50-yr-long (1950–98) AMIP integrations of NCAR's Community Atmospheric Model (CAM3.0) and NASA's Seasonal-to-Interannual Prediction Project's (NSIPP's) atmospheric model were produced

from slightly different SST analyses, as discussed in RBN.⁴ The CAM model was run at T85 spectral resolution, while the NSIPP one was integrated on a $2.0^\circ \times 2.5^\circ$ latitude–longitude grid. The eight-member NSIPP ensemble mean and the five-member CAM3.0 ensemble mean are analyzed here—an overkill, in context of seasonal variability. Note that CAM3.0 is part of NCAR's current Community Climate System Model (CCSM3.0), which is being used for characterizing global change in IPCC assessments.

North American Regional Reanalysis (NARR)

The North American Regional Reanalysis is a long-term, consistent, data-assimilation-based, climate data suite for North America (<http://www.emc.ncep.noaa.gov/mmb/rrean/>; Mesinger et al. 2004). The regional reanalysis is produced at high spatial and temporal resolutions (32 km, 45 layer, and 3 hourly) and spans a period of 25 yr from October 1978 to December 2003. It is based on the April 2003 frozen version of NCEP's mesoscale Eta forecast model and data assimilation system. As noted before, NARR assimilates precipitation unlike its global counterparts: ERA-40 (<http://www.ecmwf.int/products/data/archive/descriptions/e4/>) and NCEP reanalyses (Kalnay et al. 1996). The assimilation is, in fact, quite successful; with downstream effects, including interaction of realistic precipitation with a comprehensive land surface model (Ek et al. 2003; Mitchell et al. 2004). The NARR dataset thus appears promising in providing an improved description of land surface states, water/energy fluxes, and various atmospheric fields.

The base period for calculating seasonal climatology is 1979–98. Fields are plotted after regridding the data on to a $2.5^\circ \times 5^\circ$ latitude–longitude grid, whenever possible. Winter and summer have their usual boreal definitions: December–February and June–August, respectively.

3. Precipitation and surface air temperature variability

Precipitation and surface temperature are, perhaps, the most extensively measured hydroclimate fields, as noted earlier. Global change projections are also expressed in terms of these fields in view of their considerable influence on human activity. Both the annual-mean and annually varying components in station observations, satellite-based estimates, global and

⁴ SST differences are anticipated to be insignificant in comparison with the model structure and parameterization differences.

regional reanalyses, and atmospheric model simulations are intercompared in this section. The annually varying component is extracted from harmonic analysis of the climatological monthly means and displayed using vectors; with the length denoting the annual-cycle amplitude, and the direction its phase. The compact description is supplemented by winter and summer snapshots.

a. Precipitation distribution

The U.S.–Mexico station precipitation, shown in Fig. 1a, serves as a reference point in the ensuing comparisons. The annual mean is contoured, while the annually varying component is shown using vectors, as noted earlier. The eastern half of the continent is clearly favored in the annual-mean distribution, with rainfall of 2–3 mm day⁻¹ over the entire region. Annual rainfall amounts (~900 mm) are thus substantial, comparable, in fact, to the Indian summer monsoon rainfall totals, except that the latter are received over a shorter 3–4 month period. Meager rainfall over the western half of the continent, with wide swaths having less than 1 mm day⁻¹, along with the very wet Pacific/Northwest poignantly characterize the western water issues.

The vectors in Fig. 1a reiterate the well-known features of the seasonal distribution: the winter rainy season in the Pacific Northwest, summer rains over the Great Plains, Mexican and Central American monsoons, and the lack of a well-defined rainy season along the eastern seaboard and the U.S. Gulf Coast. The annual-cycle amplitude in the Pacific Northwest and the northern Great Plains is necessarily smaller than the annual mean, but only by about a third.⁵

Note that NARR precipitation is not shown in Fig. 1 because it is virtually indistinguishable from assimilated observations (Fig. 1a).

The CMAP-2 precipitation climatology (Fig. 1b) is similar to the station-based distribution over the United States since both share the rain gauge data. The dataset differences pale in comparison with the departures of global reanalyses from observations, especially ERA-40, where annual rainfall over the central/eastern United States is significantly smaller, by up to a third (Fig. 1c). The annual cycle is also weak, particularly, over the Great Plains. NCEP reanalysis (Fig. 1d), in contrast, depicts the eastern United States to be wet-

ter—again, by as much as a third—a well-known deficiency (Higgins et al. 1996; Trenberth and Guillemot 1998). Somewhat less well known, but an equally notable NCEP departure, is the excessive amplitude of the precipitation annual cycle across the United States, over the southeast in particular, where the observed amplitude is negligible (cf. Figs. 1a and 1b). The rainy season over the Great Plains also peaks a month earlier in the NCEP reanalysis.

Model renditions of U.S. seasonal precipitation variability are not as different as the global reanalysis representations. Both simulations have annual rainfall deficits over the central/eastern United States, but especially CAM3.0, which is closer to ERA-40 than observations. The Mexican monsoon, on the other hand, is more vigorous in both model runs, particularly, in the west, much like in the NCEP reanalysis. The winter rainy season penetrates more inland in the Pacific Northwest in both simulations, reflecting the resolution challenges of the region. Models depart from each other over the southeastern United States, where annual-cycle amplitudes are unrealistically large in the NSIPP simulation, exhibiting strong similarity with the problematic NCEP representation there. The CAM3.0 amplitudes are, comparatively, more realistic.

The summer and winter precipitation over the continent and adjoining oceans is shown in Fig. 2. The CMAP-2 distributions serve as reference points here because of land and ocean coverage. The NARR fields are displayed for the first time here. The summertime wetness over the eastern half of the continent is nicely captured in NARR and ERA-40, but the region is much too wet in NCEP. The precipitation structure over Mexico and the eastern tropical Pacific reveals varying degrees of competition between land and ocean: precipitation moves northward across most longitudes in CMAP-2, but the advance is somewhat greater over land (cf. Figs. 2a–b). The land advance is however exaggerated in global reanalyses, particularly, NCEP. Oceanic precipitation in NCEP, in contrast, shows little movement between winter and summer (cf. Figs. 2g–h), in disagreement with CMAP-2.

The winter precipitation (right column) is reasonably represented over the Pacific Northwest, but not over the southeastern United States, where global reanalyses are challenged; this time, though, the bias is dry, and equally strong in both NCEP and ERA-40 datasets. The modest annual-mean departures thus mask the considerably bigger, and oppositely signed, seasonal errors, especially, in NCEP reanalysis.

The simulated precipitation climatologies are shown in Fig. 3. The CAM3.0 distributions resemble ERA-40's

⁵ The amplitude cannot be larger than the annual mean as that would imply negative precipitation at some point in the year, unless semiannual variability is also important, which is the case in the Tropics.

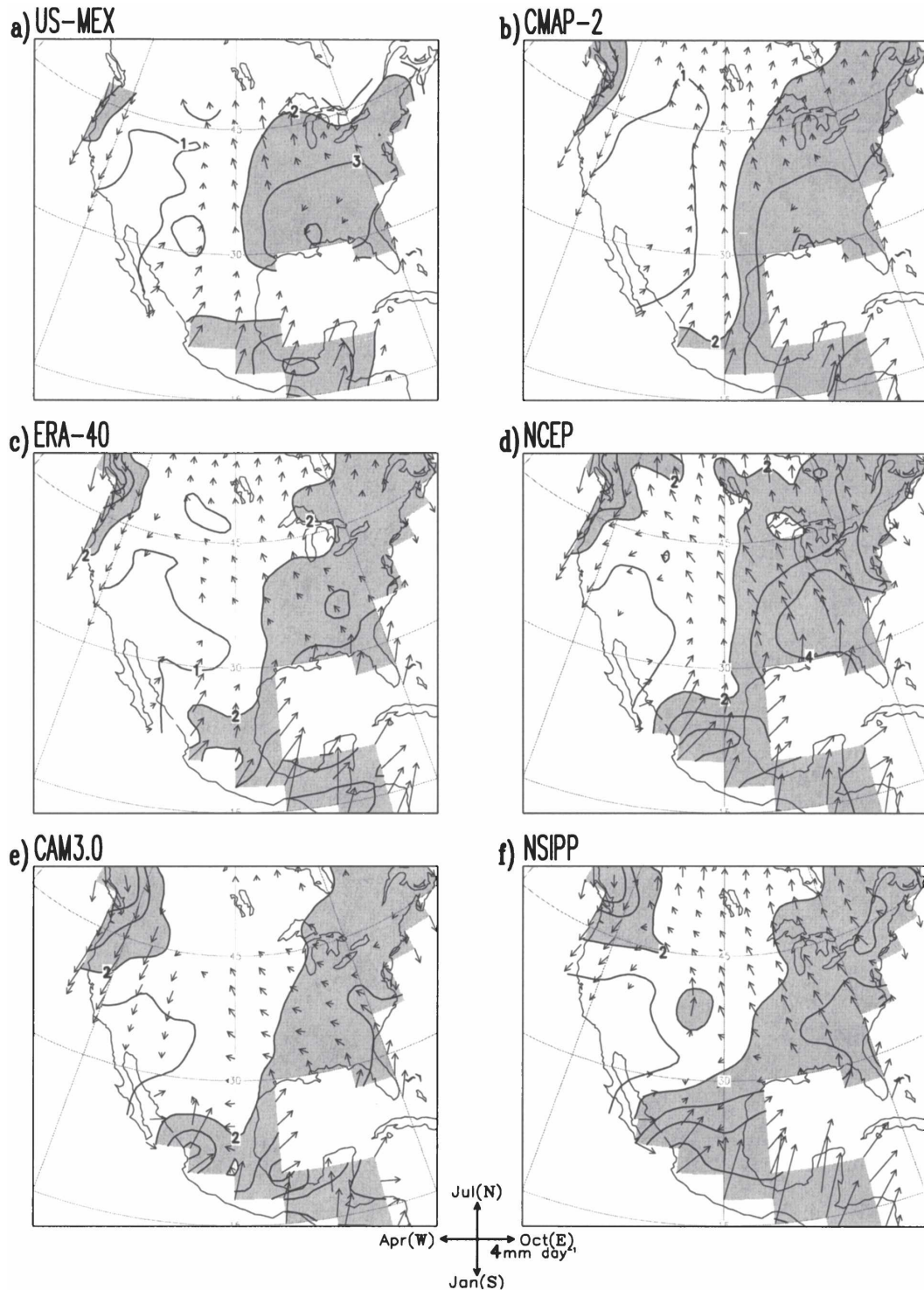


FIG. 1. Climatological precipitation (1979–98): (a) U.S.–Mexico station data, (b) satellite-based CMAP-2 analysis, (c) ERA-40 reanalysis, (d) NCEP reanalysis, (e) CAM3.0 simulation, and (f) NSIPP simulation. Vectors represent annual cycle (first harmonic) while contours show annual mean in mm day^{-1} . Vector scaling and annual-cycle phase is shown at the bottom; vectors pointing south indicate January as the maximum rainfall month, and so on. Annual-mean precipitation is contoured at 1, 2, 3, 4, 6, and 9 mm day^{-1} levels and shaded when larger than 2 mm day^{-1} . The amplitude threshold for plotting vectors is 0.5 mm day^{-1} .

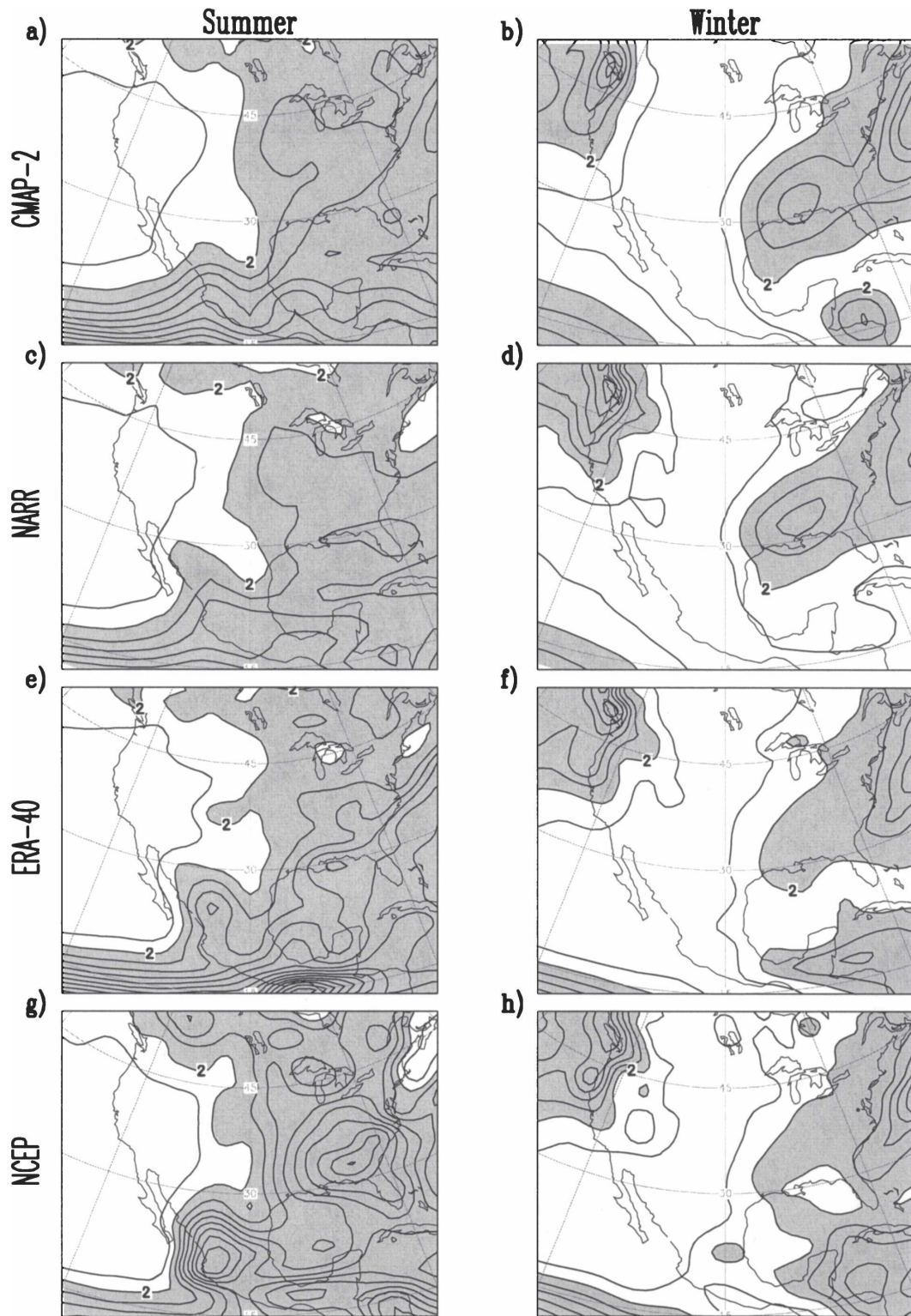


FIG. 2. Climatological (left) summer (June–August) and (right) winter (December–February) precipitation: (a), (b) CMAP-2 analysis, (c), (d) NARR reanalysis, (e), (f) ERA-40 reanalysis, and (g), (h) NCEP reanalysis. Contour interval is 1 mm day⁻¹ and shading threshold is 2 mm day⁻¹.

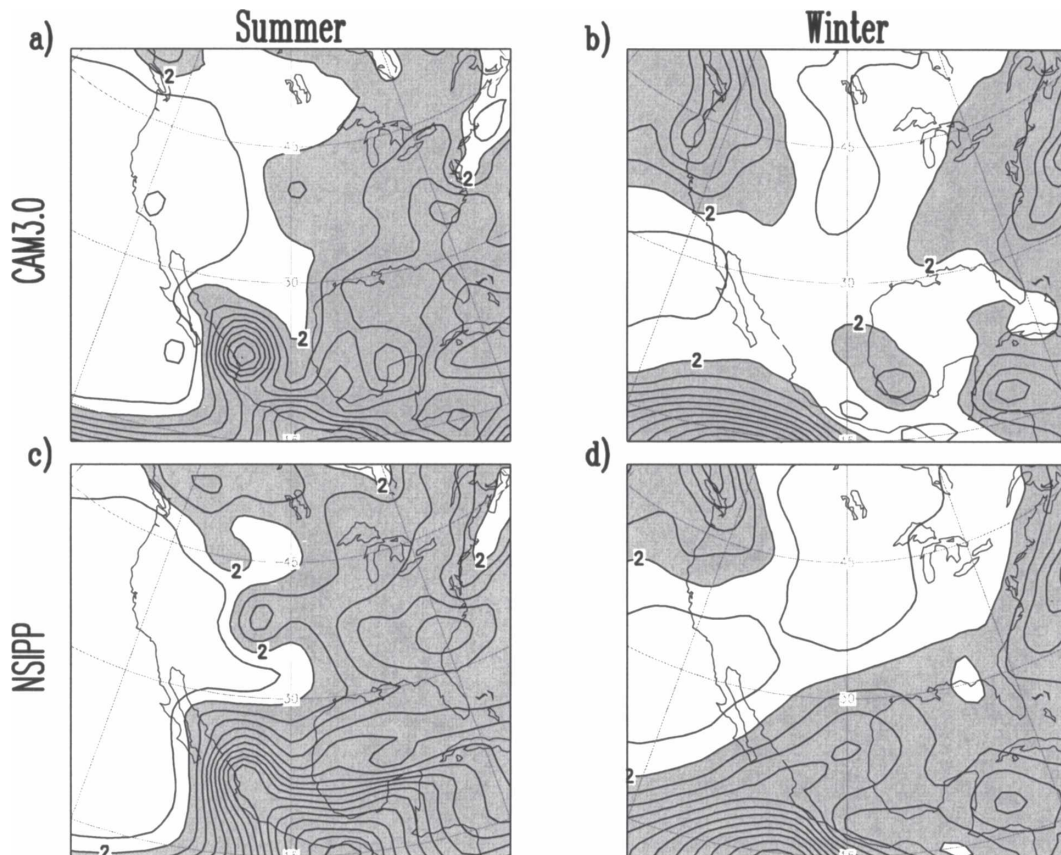


FIG. 3. Climatological summer and winter precipitation: (a), (b) CAM3.0 simulation and (c), (d) NSIPP simulation. Contour interval and shading threshold as in Fig. 2.

while the NSIPP ones are closer to NCEP's, particularly in summer. The land–ocean competition for convection is, if anything, more intense in the model Tropics: so much so that the oceanic ITCZ accompanying the phenomenally strong Mexican monsoon is located southward of its winter position in both models!⁶ Of the two, the NSIPP model is more extreme, perhaps, because of an overly responsive land surface: convection diminishes over Mexico in winter, but it doesn't abandon land as completely as it does in the CMAP-2 and NARR distributions. In contrast, the winter rainy season in the Pacific Northwest is well simulated, except for its greater inland extension. The winter rainfall maximum over the southeastern United States is how-

ever challenging for the models, much as it was for both global reanalyses. Annual-mean dryness over the Gulf Coast states in models is thus attributable to deficient winter rainfall.

The intercomparisons are not encouraging: great divergence in the representation of seasonal precipitation variability in the global reanalyses, with the models being somewhere in between, and both showing significant departures from observations. The NCEP and ERA-40 products should not be used in evaluating hydroclimate simulations, at least over the United States.

b. Surface air temperature (SAT)

The air temperature at the earth's surface is not uniquely defined (e.g., NASA Goddard Institute for Space Studies; http://data.giss.nasa.gov/gistemp/abs_temp.html). Terrain height differences arising from horizontal resolution variations can, among other things, generate artificial differences between various SAT analyses, making intercomparison daunting. Such differences can be marginalized by focusing on seasonal

⁶ This is not because of the underlying sea surface temperature, for its seasonal evolution is prescribed in the AMIP integrations. Is the ITCZ position better simulated in a more interactive modeling environment, such as those provided by coupled ocean–atmosphere models? The answer is no, at least in the case of the NCAR model.

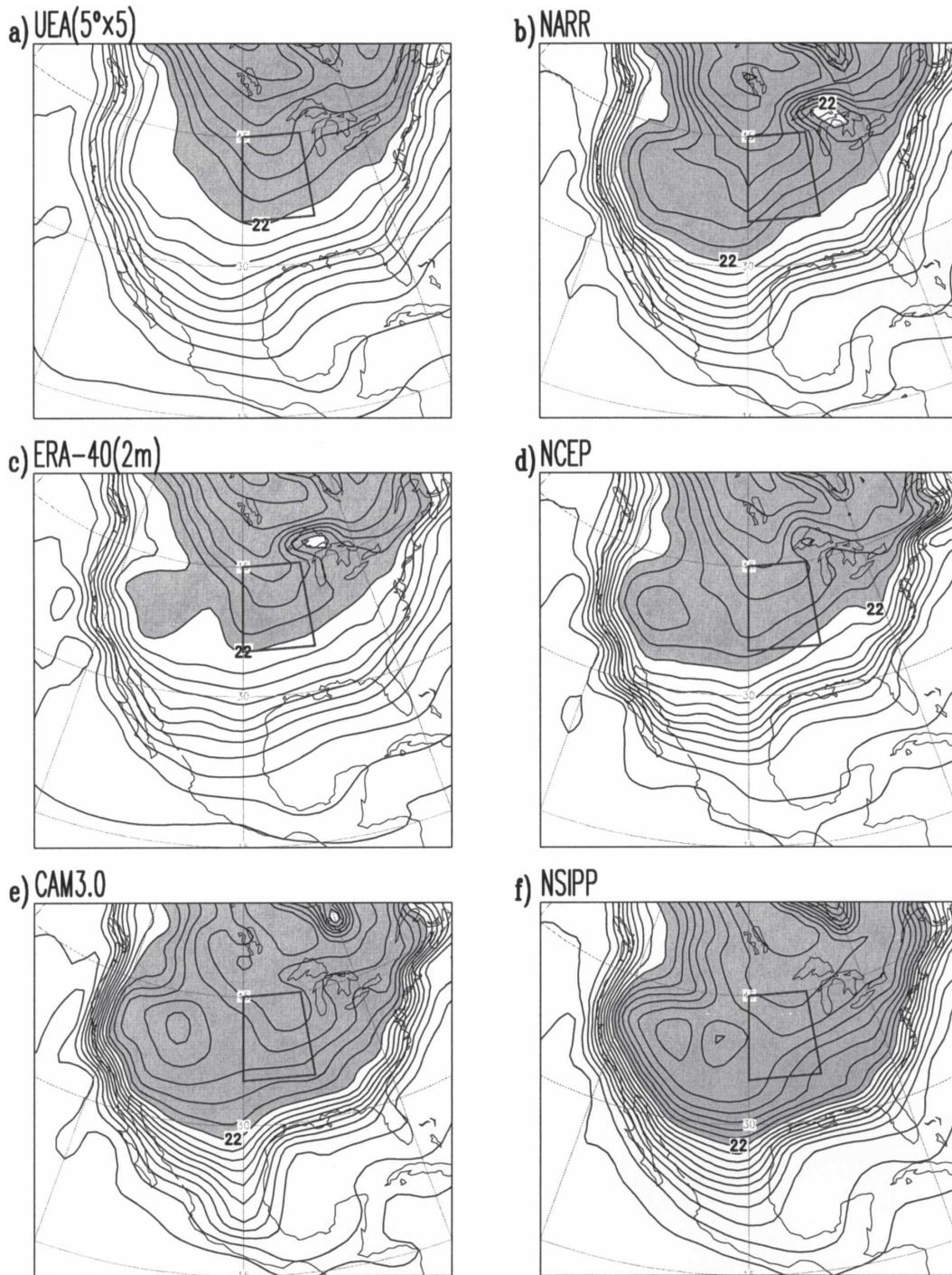


FIG. 4. Climatological SAT difference (summer minus winter): (a) UEA station data, (b) NARR reanalysis, (c) ERA-40 reanalysis (2 m), (d) NCEP reanalysis, (e) CAM3.0 simulation, and (f) NSIPP simulation. Contour interval is 2 K and shading threshold is 22 K. Box in (a) outlines the Great Plains region (35° – 45° N, 100° – 90° W) used in calculating areal averages for Fig. 5.

evolution rather than the seasonal distributions themselves: For instance, the winter-to-summer evolution, obtained by subtracting the summer and winter means, can be more readily and reasonably intercompared.

The SAT difference (summer minus winter) is displayed in Fig. 4. Datasets are plotted on the same grid, with the exception of UEA temperatures, which are on a coarser grid; values greater than 22 K are shaded in all

cases. Seasonal differences are, not surprisingly, largest in the continental interior, that is, away from the moderating influence of oceans, and in the northern latitudes where seasonal insolation changes are stronger. The contours are tightly bunched along the U.S. west coast in all panels, reflecting influence of the rapidly changing landscape, from oceanic to arid mountain ranges. Contour packing is less tight along the southern and eastern perimeter of the continent in UEA and ERA-40 distributions, in accordance with the more modest pace of landscape variations here, particularly along the eastern seaboard. Contours in CAM3.0 and NSIPP simulations (and, to an extent, NARR and NCEP reanalyses) however remain tightly bunched along the U.S. east coast, indicating some deficiency in the representation of landscape variations in this region and/or a dry bias in one of the seasons.⁷

The seasonal SAT difference is largest in the continental interior, but its amplitude varies across datasets: in the 30°–45°N sector, the winter-to-summer SAT change is in excess of 28 K in ERA-40 and UEA, reaches 30 K in NCEP, is up to 32 K in NARR and CAM3.0, and reaches as much as 36 K in the NSIPP simulation. Models are, apparently, more responsive than nature, at least, in context of seasonal SAT variability. This must have implications for the model-derived projections of global climate change, which are often couched in terms of SAT changes. The SAT average in the 10° latitude–longitude box (35°–45°N, 100°–90°W marked on Fig. 4a; box choice discussed in RBN) is shown in all calendar months, after removal of the annual mean in Fig. 5.

The SAT is lowest in January and highest in July except in the NSIPP simulation, where temperatures are highest in August. Winter temperatures are about 15 K colder than the annual mean while the summer ones are about 13 K warmer in the UEA and ERA-40 datasets,⁸ which are in accord in their portrayal. Models exhibit larger range, as noted before: a 33-K swing in CAM3.0 and a 37-K variation in NSIPP. The 5–9-K larger SAT amplitude in the models merits an investigation, especially since CAM3.0 is being used in IPCC

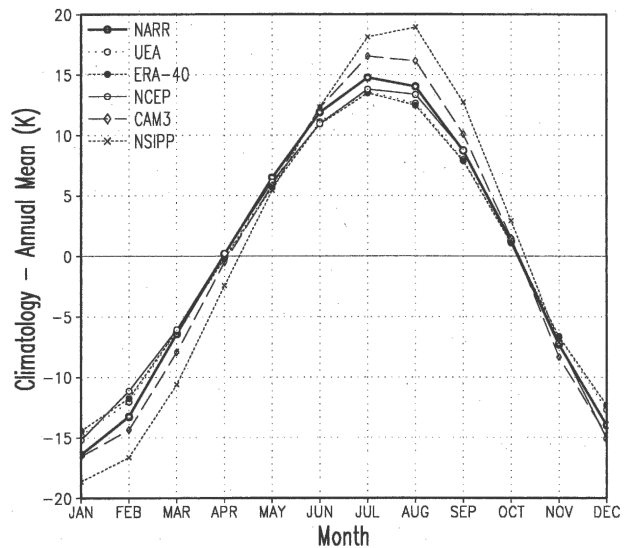


FIG. 5. Climatological SAT departure (from the annual mean) averaged over the Great Plains region. NARR: thick continuous line with circles; UEA: dotted line with circles; ERA-40: short dashed line with filled circles; NCEP: thin continuous line with circles; CAM3.0: long dashed line with diamonds; and NSIPP: short dashed line with Xs.

assessments, as part of the CCSM3.0 climate system model. Investigation of the models' overresponsiveness is however beyond the scope of this study since SAT is influenced by numerous processes, including atmosphere–land surface (vegetation) interaction and boundary layer mixing.

4. Stationary and transient moisture fluxes

Moisture fluxes, like precipitation, exhibit substantial regional and seasonal variations over the United States (Rasmusson 1967, 1968; Roads et al. 1994; Rasmusson and Mo 1996; Ropelewski and Yarosh 1998; among others). Transport by the time-averaged flow (stationary fluxes) is generally larger than that arising from correlation of moisture and wind fluctuations (transient fluxes) over North America by a factor of 5 or so, for the column average.

a. Stationary fluxes

The vertically integrated stationary moisture fluxes from the global and regional reanalyses are shown in Fig. 6; the summer fields are in the left column; flux convergence is contoured and shaded.⁹ The circulation

⁷ A dry bias over southeastern United States in the simulations (cf. Figs. 2–3) can lead to larger seasonal SAT variations. That ERA-40 and NCEP distributions exhibit a more reasonable SAT range in the presence of a similar dry bias is not disconcerting since temperature and precipitation are not tightly coupled in the reanalyses, on account of continuous assimilation of observations.

⁸ The summer warming is a bit weaker than winter cooling because insolation in summer is also used in evaporation of soil moisture (recharged over the winter-to-spring period). Land surface temperature and, consequently, SAT is thus not as warm as it could be otherwise.

⁹ The mass-weighted, vertically averaged stationary fluxes were computed from integration over the surface-to-300-hPa layer using data at the NCEP reanalysis pressure levels, in all cases. Tran-

context for the summertime stationary fluxes are the sea level pressure anticyclones stationed over the adjoining midlatitude ocean basins: the Pacific high to the west and the Bermuda high to the east.¹⁰ The Pacific high directs westerly/northwesterly flow onto the Pacific Northwest region, but with little precipitation yield, for reasons discussed later. The eastern flank of the Pacific high leads to northerlies along the U.S. west coast, but the southward moisture flux is self-limiting since the same flow also generates coastal upwelling, and thus colder sea SSTs. Colder coastal SSTs not only influence atmospheric humidity in the fetch region, but also the flow itself, particularly in the northeastern Tropics. In such subsidence zones, the zonal SST gradient, arising from colder SSTs to the east, will generate southerly flow according the Lindzen–Nigam model for tropical winds (Lindzen and Nigam 1987), opposing the primary Pacific high circulation in the northeastern tropical Pacific. Not surprisingly, southward moisture fluxes are significant only along the northern sections of the coast.

Influence of the Bermuda high is more substantial but largely confined to the eastern seaboard. The western flank of the high skirts the U.S. east coast, and its influence on seaboard precipitation must thus be through ways other than fluxing moisture to the influenced region, as discussed later in this section.

The circulation reaching the continental interior is also a coherent, large-scale, anticyclonic circulation. It comprises easterly flow over the Caribbean—part of the Atlantic trade winds—and a southerly jet leaning against the eastern slopes of the Sierra Madre Oriental range, which, together, sweep phenomenal amounts of moisture from the Gulf of Mexico and Caribbean seas northward, into the continental interior. This circulation is well represented in all three reanalyses; the NCEP representation has been noted earlier by Higgins

sient fluxes were also computed in the same manner, except in NARR, where the integration is over slightly different pressure layers. Transient fluxes are obtained indirectly in NARR, by subtracting the diagnosed stationary flux from the total flux (in the deeper surface-to-25-hPa layer), since the latter was readily available in the NARR data archives. Inclusion of the extra 300–25-hPa layer is of little consequence for moisture flux diagnosis given the rapid fall-off of moisture with height, but integration over all NARR pressure levels, particularly, the additional ones in the lower troposphere, in calculation of the total flux could result in slight overestimation of the transient component. (A direct, albeit tedious, computation of the transient moisture flux is currently underway.)

¹⁰Note that the subtropical highs are strongest and maximally extended in the northern summer season, despite a weaker summertime Hadley cell—a conundrum first addressed by Hoskins (1996).

et al. (1997, their Fig. 17d) and Trenberth and Guillemot (1998, their Fig. 9). Eastward fluxes, unrelated to this circulation, are additionally present over the northern tier states. These fluxes must develop from local evaporation of soil moisture, which gets recharged in antecedent seasons/months from precipitation and snowmelt.

Key continental features of moisture convergence include the flux divergence over northeastern Mexico and convergence to its north. The features are strongest in NCEP and weakest in NARR. A prominent NARR feature altogether missing in global reanalyses is the coherent convergence occurring over the northern Gulf of Mexico. Despite this contribution, summer rainfall over the U.S. Gulf Coast is less in NARR in comparison with global reanalyses (cf. Fig. 2). The offsetting transient contribution (shown later in Fig. 9) is one reason, but even otherwise this would not be surprising as NARR's atmospheric water budget is unbalanced on account of ongoing precipitation assimilation. NARR differs from the global reanalyses also in the eastern tropical Pacific: fluxes in the ITCZ's northern flank are divergent in NARR but convergent in others, for reasons that are unclear.

The continental interior is a quiescent region in winter from the viewpoint of flux activity. Stationary moisture fluxes (right panels) are significant mostly along the East and West Coasts, reflecting the influence of circulation features in the adjoining basins; this time, though, it is the sea level pressure cyclones: Aleutian low in the north Pacific and the Icelandic low in the north Atlantic. Fluxes in the interior are nondescript except for the eastward ones over eastern United States. These fluxes, especially those in the northeastern corner must arise, in part, from the Icelandic low's influence. The winter fluxes exhibit greater similarity than their summer counterparts in Fig. 6 because atmosphere–land surface interactions, whose model representation is challenging (and thus varied), are relatively muted in winter.

The simulated stationary moisture fluxes are shown in Fig. 7. Notable midlatitude features, including flux convergence over the northern Great Plains in summer and the Pacific Northwest in winter are modeled well. Subtropical features are not as well captured, though: westward fluxes over the Gulf of Mexico and Caribbean seas in summer are not as tightly confined, meridionally, as in reanalyses, for example. In the Tropics, the models are clearly challenged, particularly over oceanic regions, despite the specification of seasonally evolving SSTs in the simulations. Both models produce flux convergence over the eastern tropical Pacific in winter, in variance with reanalyses. Land–ocean competition for

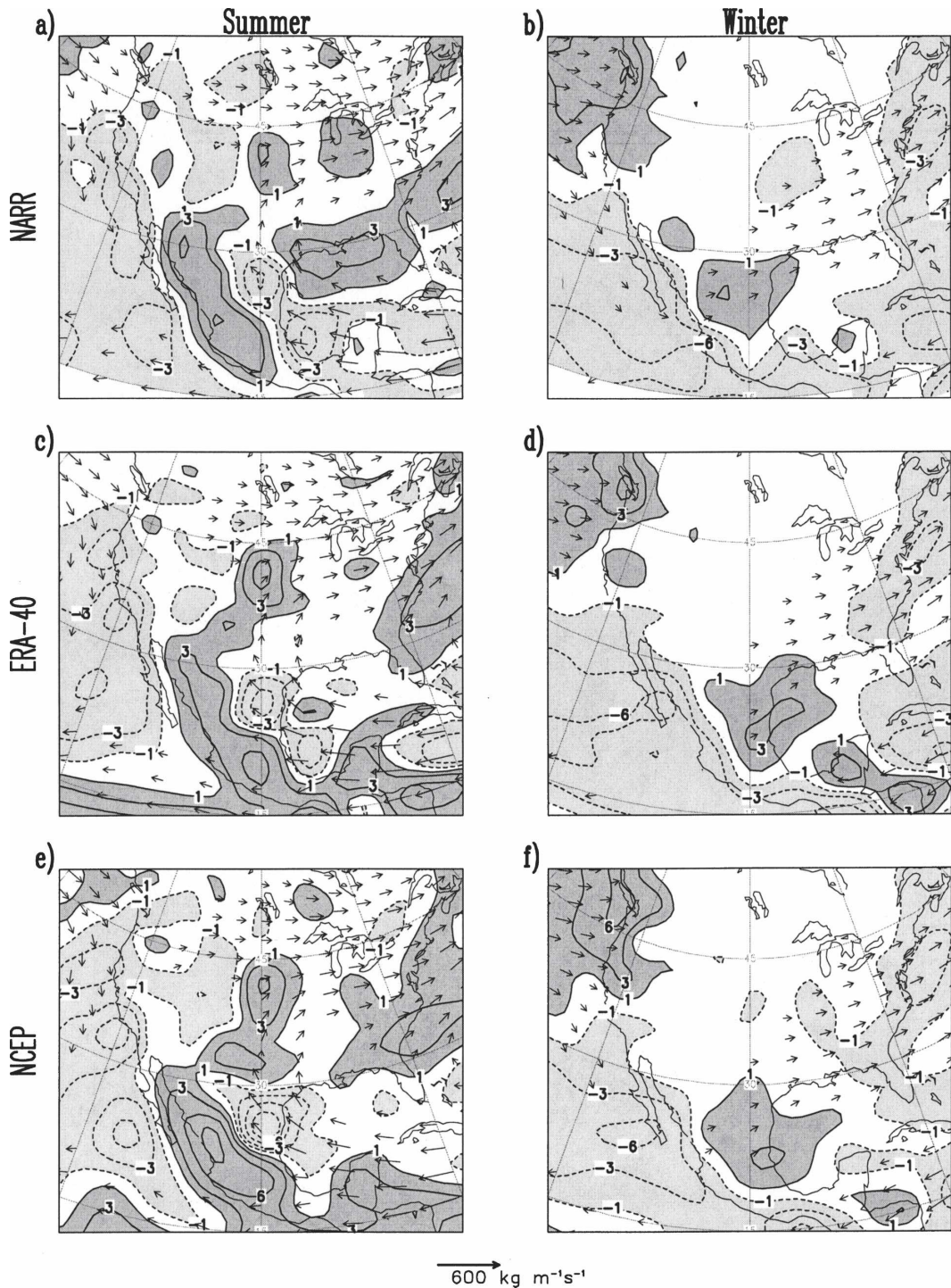


FIG. 6. Climatological stationary moisture fluxes (vertically integrated) and their convergence: (left) summer and (right) winter. (a), (b) NARR reanalysis, (c), (d) ERA-40 reanalysis, and (e), (f) NCEP reanalysis. Vector scale is indicated at the bottom, and the plotting threshold is $80 \text{ kg m}^{-1} \text{ s}^{-1}$. Moisture flux convergence is contoured using $\pm 1, 3, 6, 9, 12, 15,$ and 18 mm day^{-1} isolines. Dark (light) shading denotes convergent (divergent) regions.

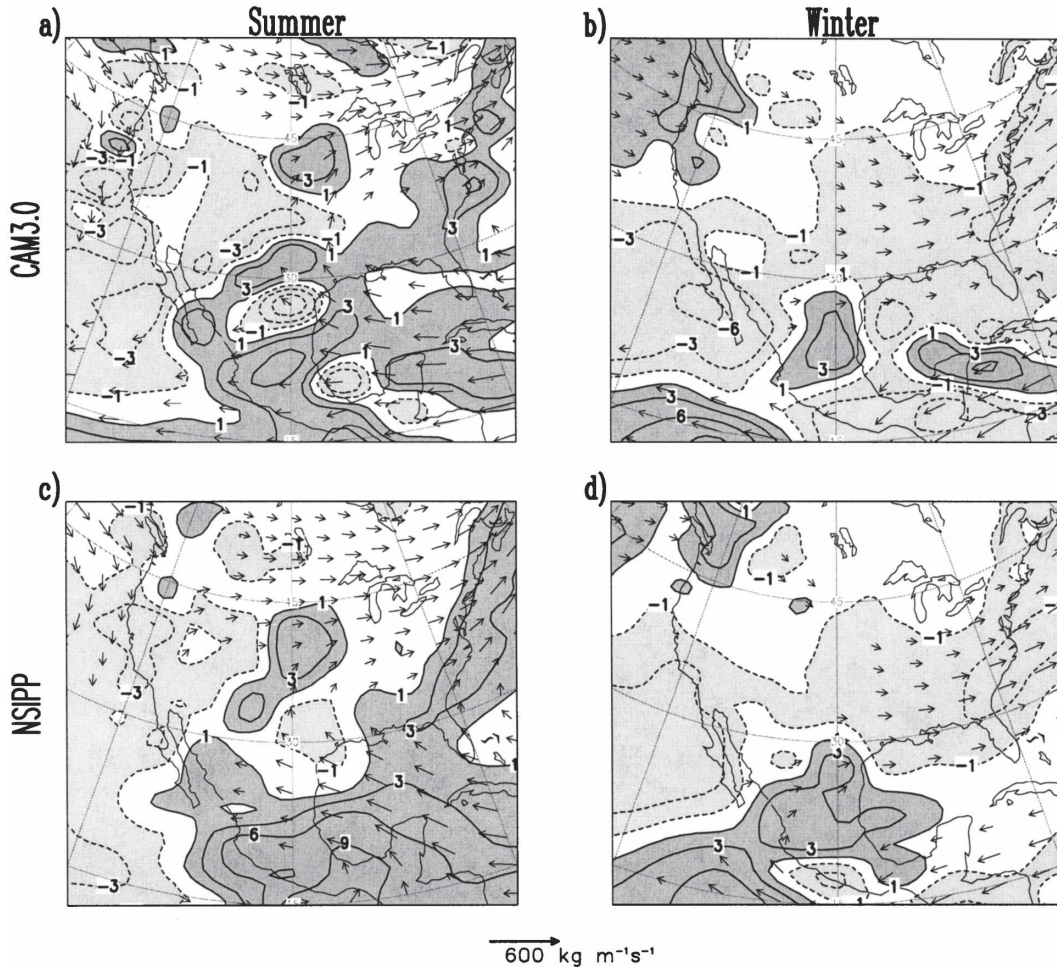


FIG. 7. Climatological stationary moisture fluxes (vertically integrated) and their convergence: (left) summer and (right) winter. (a), (b) CAM3.0 simulation and (c), (d) NSIPP simulation. Plotting and shading conventions as in Fig. 6.

convection is more intense in models, especially, NSIPP, as noted earlier. The CAM3.0 simulation is overall better than NSIPP's.

b. Summertime low-level jet

The low-level jet (LLJ) and the extent of overlap with the Bermuda high's western flank are shown in Fig. 8. The stationary meridional moisture flux in summer is displayed at a latitude grazing the U.S. Gulf Coast (30°N), with reanalysis fields in the left column. The jet core is located on the eastern slope of the Sierra Madre Oriental range in all panels. The northward moisture fluxes are strongest in NCEP, by about 25% with respect to NARR and ERA-40.

The reanalyses differ somewhat more in the representation of the Bermuda high's western arm, which skirts the U.S. east coast, and which has maximum northward fluxes at the surface. The vertical extent of

this feature and the core flux magnitude differ, with NARR exhibiting the deepest structure and strongest fluxes. The LLJ and the Bermuda high's western flank are reasonably resolved in all three reanalyses.

The simulated features are shown in the right panels of Fig. 8. The LLJ is modeled well in CAM3.0 but not in the NSIPP simulation, where the jet is too shallow and quite weak. Both simulations are however unable to adequately resolve the separation of the LLJ and Bermuda high's western arm, especially NSIPP, where the features meld into each other. This could be attributed to insufficient model resolution except that structures are more diffused in the higher-resolution simulation (NSIPP).

c. Transient fluxes

The vertically integrated transient moisture fluxes are displayed in Fig. 9, using a vector scale that is one-

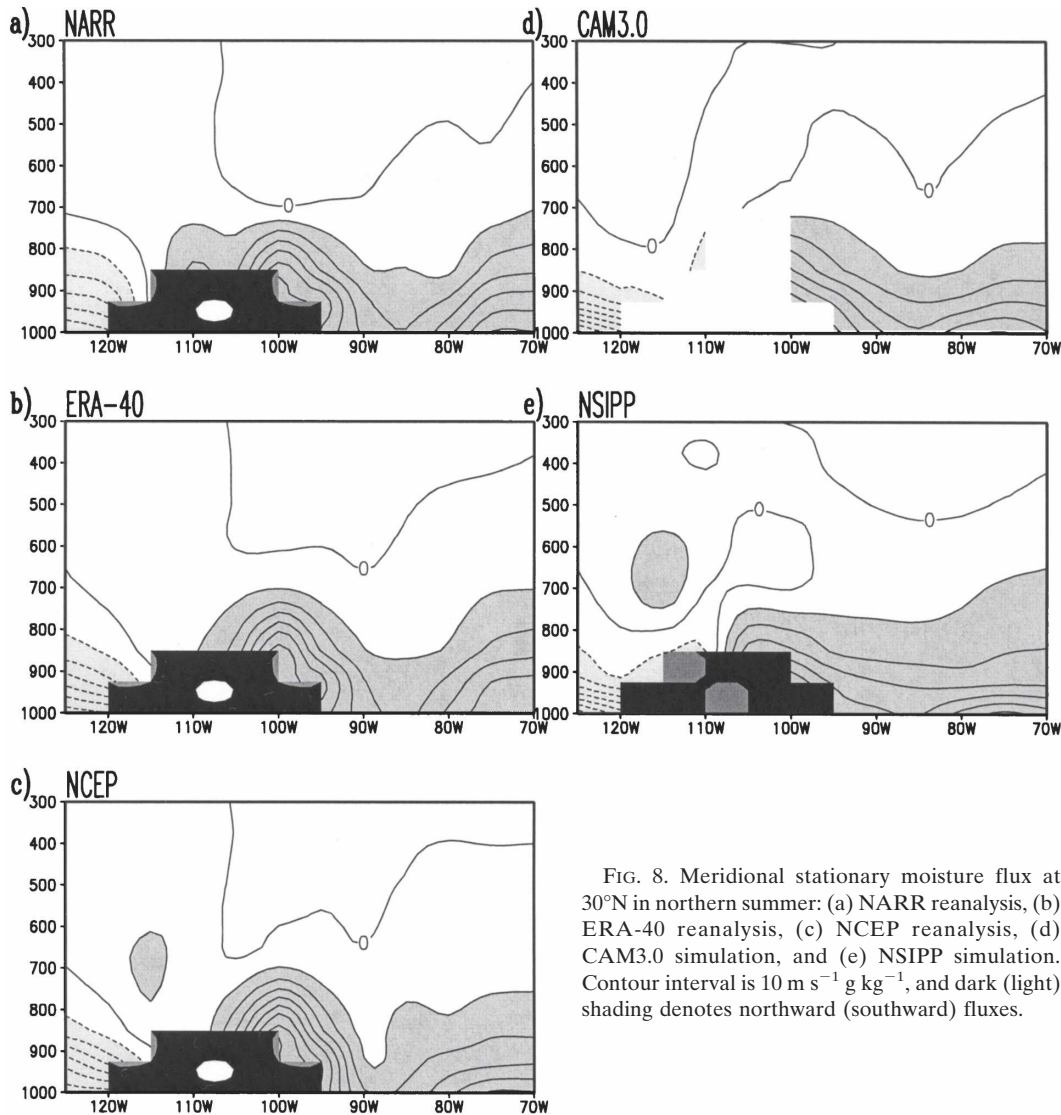


FIG. 8. Meridional stationary moisture flux at 30°N in northern summer: (a) NARR reanalysis, (b) ERA-40 reanalysis, (c) NCEP reanalysis, (d) CAM3.0 simulation, and (e) NSIPP simulation. Contour interval is $10 \text{ m s}^{-1} \text{ g kg}^{-1}$, and dark (light) shading denotes northward (southward) fluxes.

sixth of that used for stationary fluxes. Transient fluxes are oriented, primarily, northward, in contrast with the stationary ones, which are more eastward tilted, except in vicinity of the LLJ. Despite the magnitude and orientation differences, transient flux convergence is comparable to the stationary one, and often, offsetting, as in summer. Transient fluxes are particularly large over the eastern half of the continent in winter, when they determine regional moisture flux convergence; stationary fluxes, on the other hand, are more consequential in summer.

The summertime fluxes are quite similar in the global reanalysis, but fluxes in NARR emanate from the U.S. Gulf Coast rather than the Great Plains. The Gulf Coast emanation almost completely offsets the strong convergence of stationary fluxes here (cf. Fig. 6a). Flux convergence over California is also greater in NARR.

Interestingly, convergence over the Pacific Northwest shows little variation with season, attesting to the importance of stationary fluxes for the local winter rainy season; this assessment is supported by both global and regional reanalyses. Winter flux distributions are in greater accord, as before.

Transient fluxes are available only from the NSIPP simulation and are displayed in Fig. 10. Comparison with reanalyses shows the model fluxes (and convergence) to be weaker in both seasons, but otherwise realistically distributed, especially over the eastern United States.

d. Winter rainy season in the Pacific Northwest

The Pacific Northwest is under the influence of southwesterlies in winter, as opposed to northwesterlies

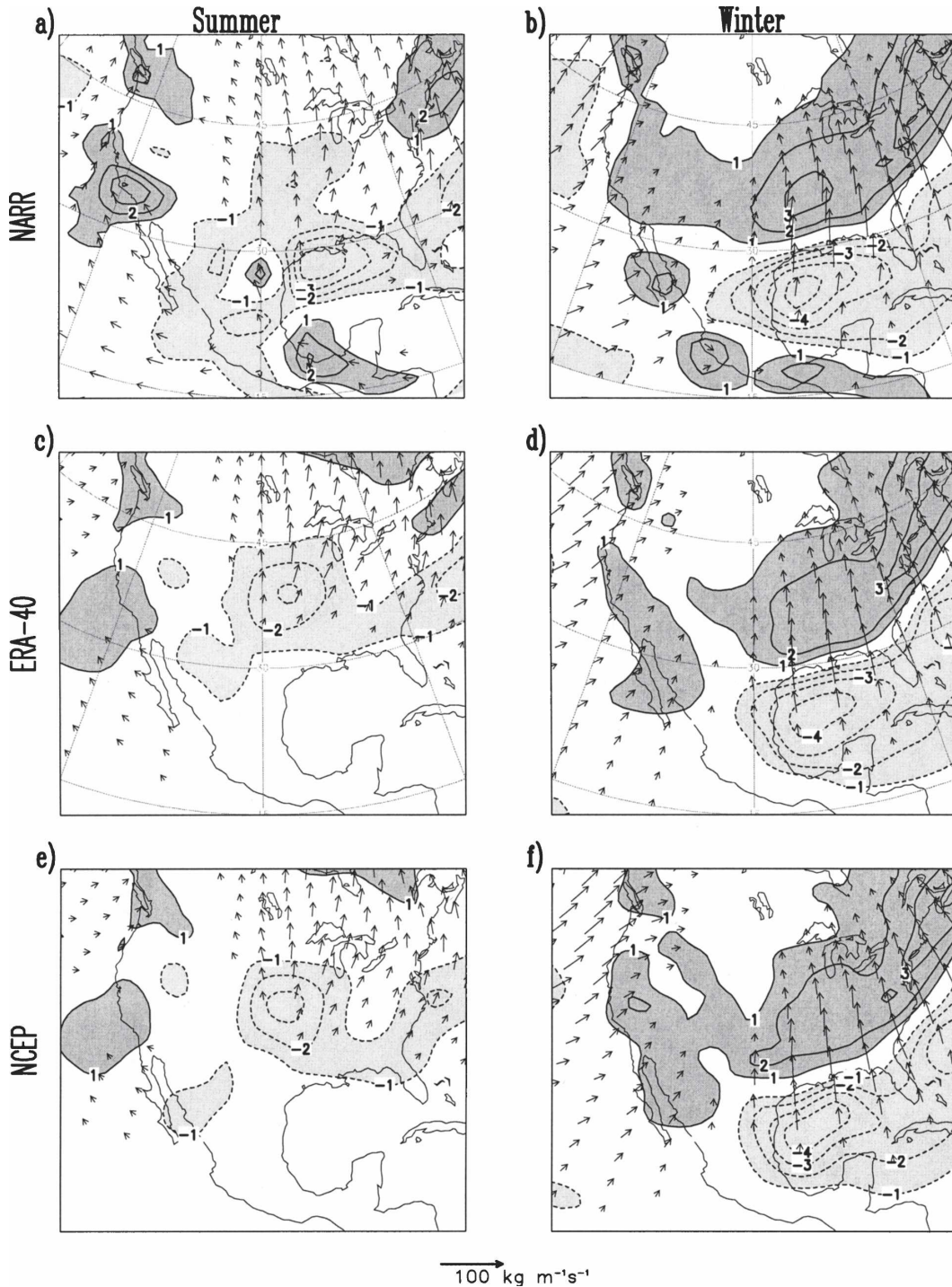


FIG. 9. Same as in Fig. 6, but for transient moisture fluxes. Note that it is one-sixth of that used for displaying stationary fluxes; plotting threshold here is $10 \text{ kg m}^{-1} \text{ s}^{-1}$.

in summer. Is the meridional direction of flow consequential for rainfall, given that winter is the rainy season here? One might expect southwesterly flow to be richer in moisture, but the two fluxes are, evidently,

comparable (cf. Fig. 6). So why is winter the rainy season in the Pacific Northwest? The region certainly is in the path of storms—more so in winter. Transient fluxes are indeed stronger in winter (cf. Fig. 9), but their con-

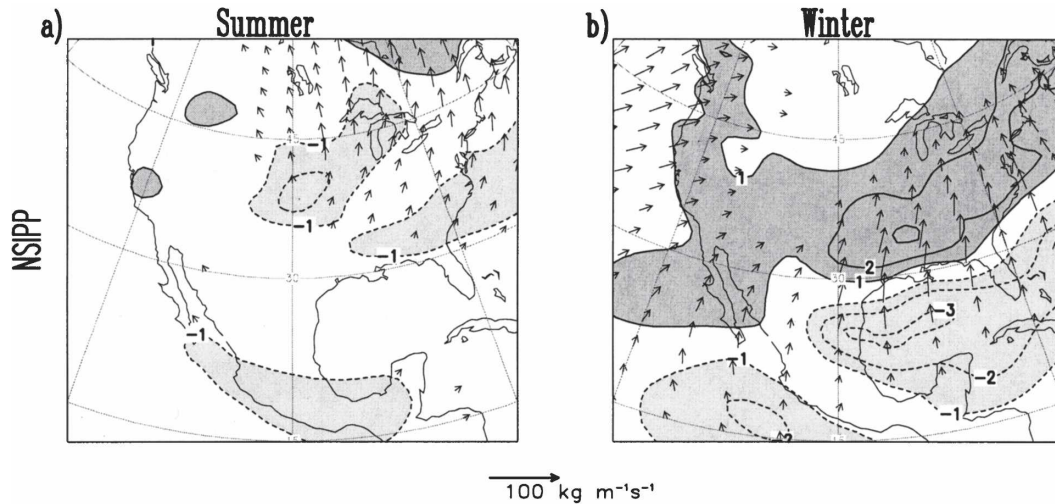


FIG. 10. Climatological transient moisture fluxes (vertically integrated) and their convergence in the NSIPP simulation: (a) summer and (b) winter. Transient fluxes were not available in the CAM3.0 monthly archives. Plotting and shading conventions are as in Fig. 9.

vergence is not; seasonal insensitivity of the convergence was noted above. Transient fluxes, in fact, contribute no more to winter moisture convergence than the stationary component, if even that much.

Interestingly, vorticity balance considerations (and induced vertical motions), rather than moisture transport ones, suggest a plausible hypothesis: The vorticity equation for steady, large-scale circulations, such as the Pacific high, reduces to one of Sverdrup balance: $\beta v \approx f \partial w / \partial z$. Planetary vorticity advection ($-\beta v$) is positive (negative) on the eastern flank of the anticyclone (cyclone). Sverdrup balance then requires that a fluid column shrink (stretch) in the vertical in the Northern Hemisphere ($f > 0$) to compensate for the advective changes, so that steady circulation can be maintained. The eastern flank of a large-scale anticyclone (cyclone) is therefore associated with divergence (convergence) and subsiding (ascending) motions. The dynamically induced vertical motions, apparently, provide an explanation for the winter rainy season in the Pacific Northwest, especially since stationary moisture fluxes contribute more than half of the total rainfall.

Can the above hypothesis also explain the structure of seasonal precipitation variability along the East Coast? The eastern seaboard is under the influence of the Bermuda high in summer, as noted earlier. The high's western flank is associated with convergence and ascending motions, by the above reasoning. The large-scale ascent should provide a conducive environment for convergence of moisture fluxes, including those due to the anticyclone itself, leading to rainfall. The hypothesis thus seems to have met its first test!

5. Summer evaporation

Evaporation is a leading component of the atmospheric water cycle over the central and eastern United States during summer, but its measurements are extremely limited, and in any case, insufficient to characterize its regional-to-subcontinental-scale variability. Evaporation is thus estimated—backed out—from both inline and offline analysis. Inline diagnosis includes the effects of two-way atmosphere–land surface interaction—a plus. Obtained estimates can however still be off the mark if the internally generated precipitation is unrealistic. Atmospheric reanalysis is an example of inline diagnosis. Offline diagnosis (Huang et al. 1996; Dirmeyer and Tan 2001), typically, provides more constrained estimates since the land surface model is driven by observed precipitation and temperature in this scheme. Land surface's feedback to the atmosphere is not factored into the offline-produced estimates.

The NARR precipitation assimilation strategy seizes on the advantages of the above approaches, but the obtained evaporation (or soil moisture) estimates are not assured to be realistic. Realism would have been assured if the land surface was entirely driven by the atmosphere in nature. This, surely, is not always the case, but NARR does adopt this very viewpoint in crafting its assimilation strategy—perhaps, out of necessity. Precipitation assimilation in NARR is accomplished by nudging precipitation, moisture, temperature (diabatic heating), and cloud water mixing ratio, *but not evaporation* (i.e., soil moisture). Land surface's influence on precipitation, through evaporation, is thus

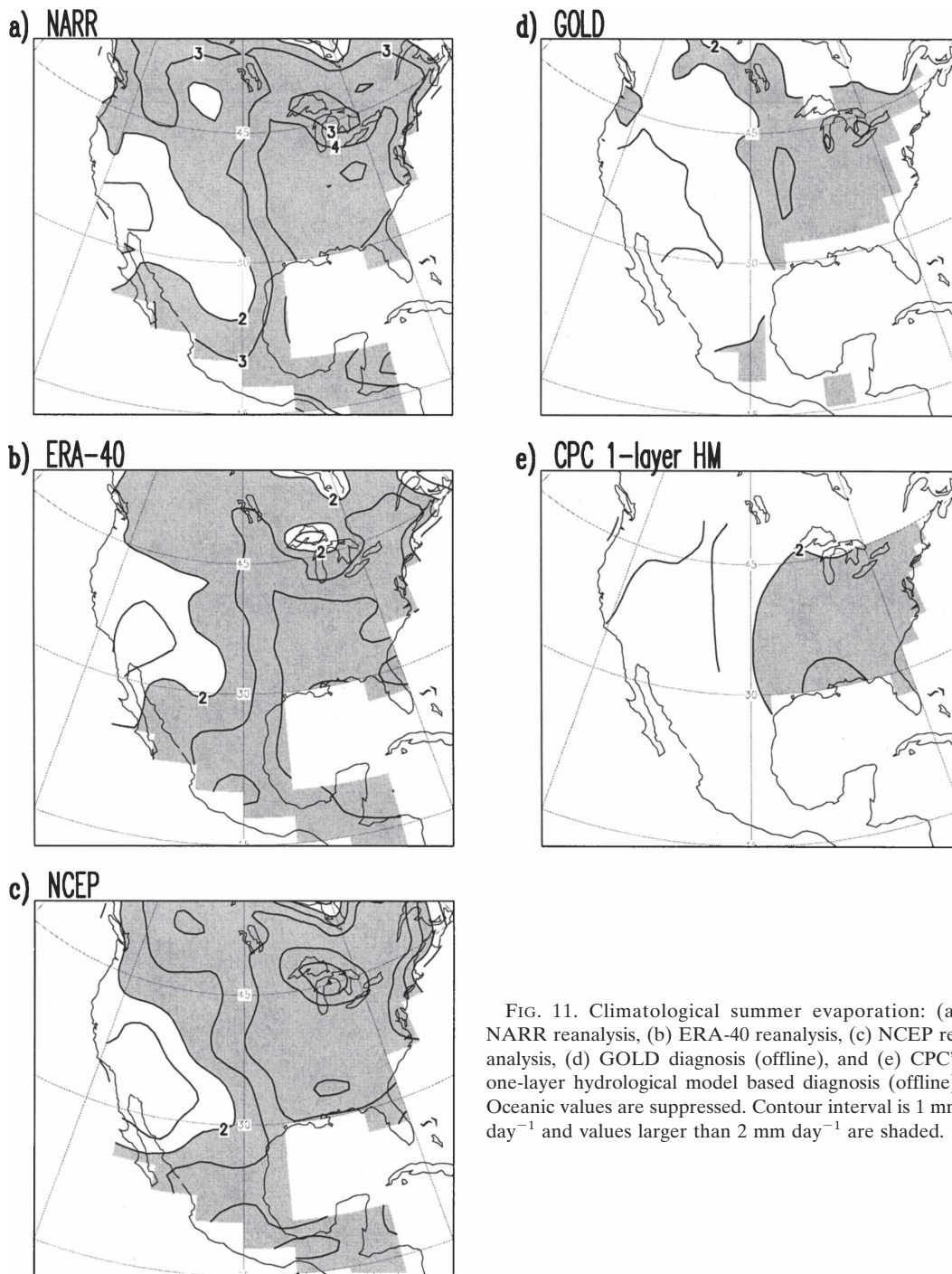


FIG. 11. Climatological summer evaporation: (a) NARR reanalysis, (b) ERA-40 reanalysis, (c) NCEP reanalysis, (d) GOLD diagnosis (offline), and (e) CPC's one-layer hydrological model based diagnosis (offline). Oceanic values are suppressed. Contour interval is 1 mm day⁻¹ and values larger than 2 mm day⁻¹ are shaded.

ignored during the assimilation process, and this is not without consequence for the atmospheric water balance, as discussed later. As such, NARR evaporation should not necessarily be deemed to be a superior estimate.

Summer evaporation in the reanalyses is shown in Fig. 11. The fields are similar, but the evaporation am-

plitude varies, being weakest in ERA-40 and strongest in the NCEP reanalysis: for example, near the 100°W meridian (Great Plains region), evaporation is 3 mm day⁻¹ in both ERA-40 and NARR but almost 4 mm day⁻¹ in NCEP, with precipitation being no more than 3 mm day⁻¹ in any of the reanalysis (cf. Figs. 2b–d). Over the southeastern United States, evaporation is

typically 4 mm day^{-1} , but rainfall is closer to 3 mm day^{-1} in NARR and ERA-40, and phenomenally large in NCEP ($\sim 6 \text{ mm day}^{-1}$). Evaporation thus exceeds precipitation over much of the central and eastern United States. The combined stationary and transient moisture flux convergence is much weaker in comparison, and slightly negative. The summertime atmospheric water balance in the reanalyses can thus be described as precipitation \approx evaporation.

Offline diagnoses (right panels) however yield smaller evaporation, with typical values being only 2 mm day^{-1} over the eastern United States, or about half of the inline estimates. These evaporation estimates are smaller than precipitation (cf. Fig. 2a), and the summer water balance according to them is precipitation \geq evaporation.

Summer evaporation in the atmospheric simulations is shown in Fig. 12. The model fields exhibit greater differences than seen in their reanalysis counterparts: evaporation over the southeastern United States is $\sim 3 \text{ mm day}^{-1}$ in CAM3.0 but almost 5.0 mm day^{-1} in the NSIPP model. CAM3.0 evaporation is thus somewhere in between the weakest inline and the strongest offline estimate, whereas NSIPP is closer to the strongest estimate.

Climatological evaporation in atmospheric model simulations cannot thus be characterized as excessive, at least in comparison with the reanalysis fields—in CAM3.0, in particular. It is interesting that these very simulations produce very large evaporation anomalies over the Great Plains in context of interannual variability— anomalies larger than both offline and inline estimates, by a factor of up to 4 (RBN). Models' propensity to recycle precipitation over the Great Plains, manifest in analysis of interannual variability, is not apparent in the climatological context, unless offline evaporation estimates are considered more realistic than the inline ones.

6. Atmospheric water cycle over the Great Plains

Portrayal of the atmospheric water cycle is completed in this section by augmenting its winter and summer description with the transition season structure of moisture flux convergence and evaporation. In the interest of space, areal averages over the Great Plains are shown in Fig. 13, at monthly resolution. The water cycle terms are plotted using the same vertical scale so that the nature of atmospheric water balance can be visually assessed. Examination of precipitation evolution (Fig. 13a) shows the reanalyses and model simulations to be in agreement in winter and early spring, but not at other times, particularly, autumn, when models (and even

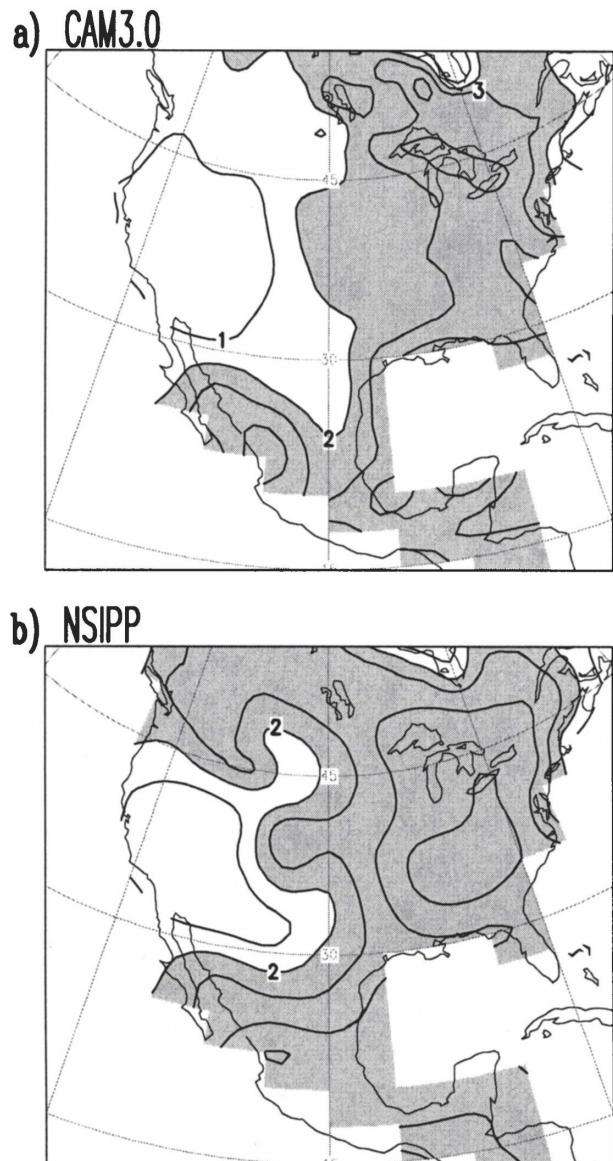


FIG. 12. Same as in Fig. 11, but for (a) CAM3.0 simulation and (b) NSIPP simulation.

global reanalyses) underestimate precipitation by a factor of up to 2. The NCEP precipitation is, apparently, excessive not only in summer, as noted earlier, but also in spring (cf. Fig. 16 of Higgins et al. 1997). The year-round dry bias of ERA-40 with respect to NARR precipitation is also noted.¹¹

Evaporation estimates (Fig. 13b) are evidently more uncertain, in part because of the large disparity be-

¹¹ U.S.–Mexico station precipitation is not plotted in Fig. 13a to avoid clutter as it is indistinguishable from NARR, a reflection of successful assimilation of precipitation in NARR.

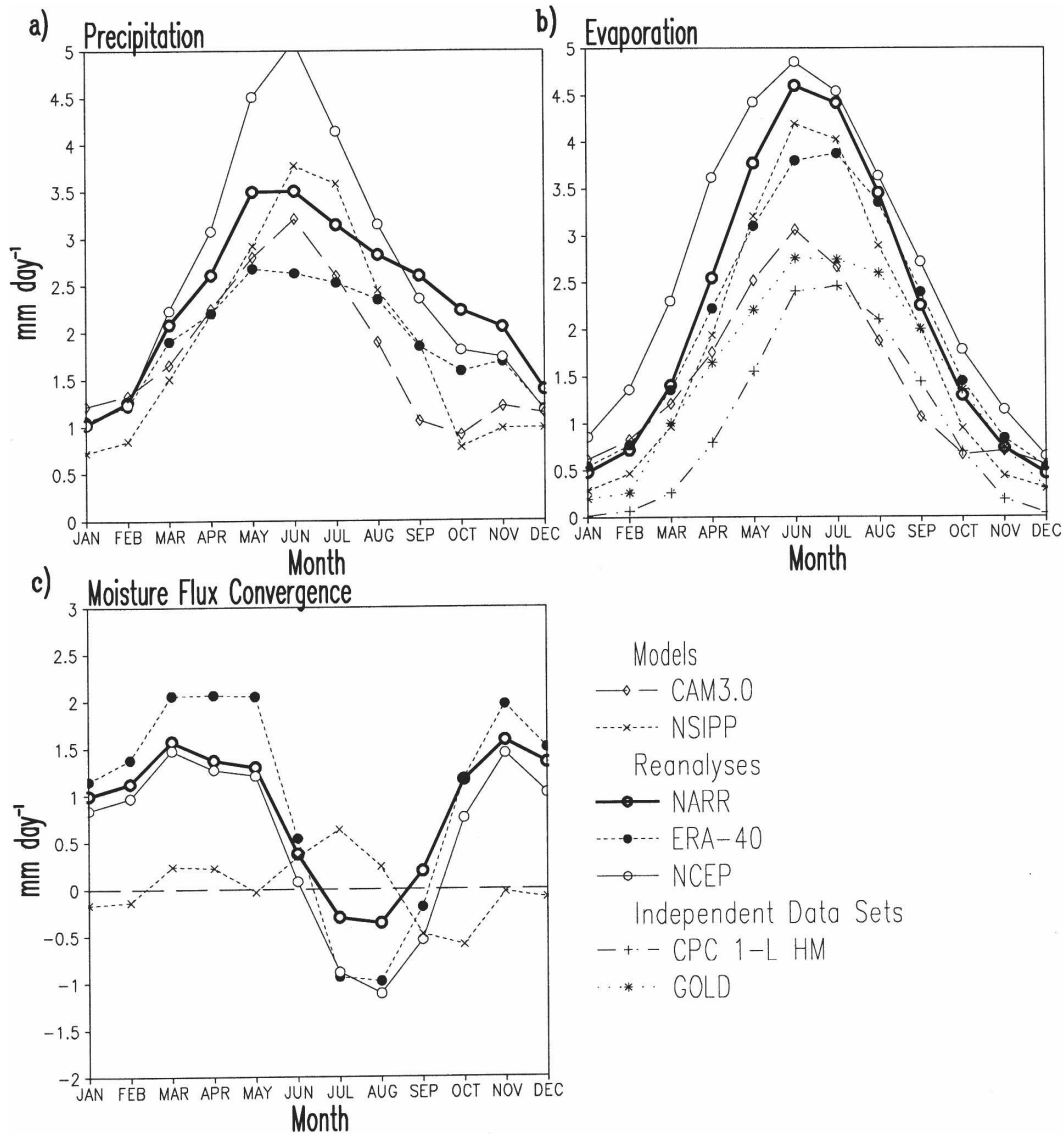


FIG. 13. Atmospheric water cycle over the Great Plains (climatology) in mm day^{-1} : (a) P , (b) E , and (c) moisture flux convergence (vertically integrated). NARR: thick continuous line with circles; ERA-40: short dashed line with filled circles; NCEP: thin continuous line with circles; CAM3.0: long dashed line with diamonds; NSIPP: short dashed line with Xs; CPC: dot-dot-dash line with plus signs; and GOLD: dotted line with asterisks.

tween inline and offline diagnoses, especially in summer when inline estimates are 50%–75% larger; differences are minimal—near zero—in autumn. Surprisingly, the spread is significant even in winter when near-zero field values lead to an expectation of consistency. Note, NCEP evaporation is an outlier in all months, not just in summer. A comparison of Figs. 13a and 13b shows that precipitation is generally larger than evaporation during October–April, while the opposite is true in other months. Model evaporations also exhibit considerable spread: CAM3.0 is closer to offline estimates, while NSIPP is nearer to the inline ones.

Evolution of moisture flux convergence over the Great Plains is shown in Fig. 13c; the sum of vertically integrated stationary and transient contributions is displayed. The reanalyses provide a consistent description of seasonal changes, particularly timing: flux convergence is important in generation of October–March precipitation, with a 1.0–1.5 mm day^{-1} contribution. Evaporation picks up notably in April and becomes the leading contributor thereafter, until September, except according to CPC’s diagnosis. During summer, fluxes are actually divergent over the Great Plains, offsetting the evaporation contribution; the divergence and the

resulting offset is somewhat weaker in NARR though.¹² ERA-40, on the other hand, exhibits large seasonal change in flux convergence.

Flux convergence in the NSIPP simulation is also plotted in Fig. 13c. Both amplitude and the sign of modeled convergence is at variance with the reanalysis distributions. Fluxes are convergent in summer, when evaporation is already larger than precipitation (cf. Figs. 13a–b). Prospects for ascertaining the nature of atmospheric water balance are thus no brighter for model simulations than they are for reanalysis datasets. The imbalance in the latter is, of course, a by-product of intermittent data insertion and the resulting dynamic and thermodynamic adjustments. Model simulations are, however, not handicapped in this way, leading to an expectation of balanced budgets in the simulations.

Atmospheric water balance over the Great Plains

The nature of atmospheric water balance is probed in this section, notwithstanding the dim prospects of finding a balanced moisture equation in reanalysis and simulation datasets. The focus is on the recently released global and regional reanalyses: ERA-40 and NARR. The vertically integrated moisture equation is $\partial W/\partial t + P - E = \text{MFC}$, where $\partial W/\partial t$ is the change in atmospheric moisture storage (typically, small), P is precipitation, E is evaporation, and MFC is the moisture flux convergence. When storage is small, $(P - E) \approx \text{MFC}$. Both sides of the approximate equality and their difference are plotted in Fig. 14. Although the terms evolve similarly in both ERA-40 and NARR in that both are positive in the early part of the year, negative during summer, and again positive in autumn/winter, the amplitude differences are overwhelming, especially in ERA-40. The amplitude discrepancy is evidently largest in late spring and the early summer months, reaching 1.5 mm day^{-1} in NARR and 2.5 mm day^{-1} in ERA-40.

The water budget imbalance in the NSIPP simulation provides a measure of tolerance in atmospheric water balance assessments. Imbalance in the simulation, which has no physical sources/sinks of water, must result from model and diagnostic analysis numerics.

The NARR budget is probed further in order to understand the origin of water imbalance in the regional model's atmosphere. The key source of imbalance is evaporation in the authors' opinion. This field (or soil

moisture) is not adjusted during assimilation of precipitation, as noted before. The assimilation procedure is also not cognizant of MFC, another important atmospheric water balance term. The procedure is, in fact, very columnar—as it, perhaps, must be—and focuses only on thermodynamics of the atmospheric column, paying no regard to dynamics (circulation and fluxes) and the underlying land surface processes (e.g., E).

For illustration purposes, consider the assimilation process when the model precipitation needs to be reduced over a certain grid box. In current implementation, the storage term ($\partial W/\partial t$) is bearing the entire burden of precipitation reduction, from perspective of the water budget.¹³ Why should this be the case? Although it is not obvious how the precipitation decrement should be apportioned between E , MFC, and $\partial W/\partial t$, putting it all on $\partial W/\partial t$ seems arbitrary. The first two terms should also be in play. Modulation of evaporation (surface latent heat flux) during assimilation seems reasonably straightforward to implement, but the same cannot be said for modulation of moisture flux convergence. Clearly, more analysis will be needed to devise an effective assimilation strategy.

7. Discussion and concluding remarks

The study has focused on the seasonal variability of the North American hydroclimate. Seasonal rhythms are monotonous and potentially uninteresting but for the complexity of their spatial footprint, especially in hydroclimate fields, such as precipitation. The complexity arises from regional ocean–atmosphere–land surface interactions, whose presence in reanalyses and model simulations can, often, only be inferred.

The study is motivated by the recent availability of a potentially improved hydroclimate analysis over North America (NARR), from a high-resolution, precipitation-assimilating regional model. This offers unique opportunities for evaluation of the hydroclimate component of *global* reanalyses; for assessment of atmospheric model simulations, particularly, fields other than precipitation and surface air temperature (for which validating observations already exist); for characterization of the atmospheric water cycle over the Great Plains, to the extent permitted by unbalanced budgets in data-assimilated products; and for advancing understanding of the spatiotemporal distribution of precipitation itself, for example, the winter rainy season in the Pacific Northwest. The main findings are as follows:

¹² NARR's summer moisture flux divergence is also weak in comparison with the radiosonde based estimate (1973–92; Ropelewski and Yarosh 1998), which is closer to 1.0 mm day^{-1} , that is, to the global reanalysis value.

¹³ Latent heating and cloud water mixing ratio are also adjusted during precipitation assimilation to account for the energy implications of precipitation adjustment.

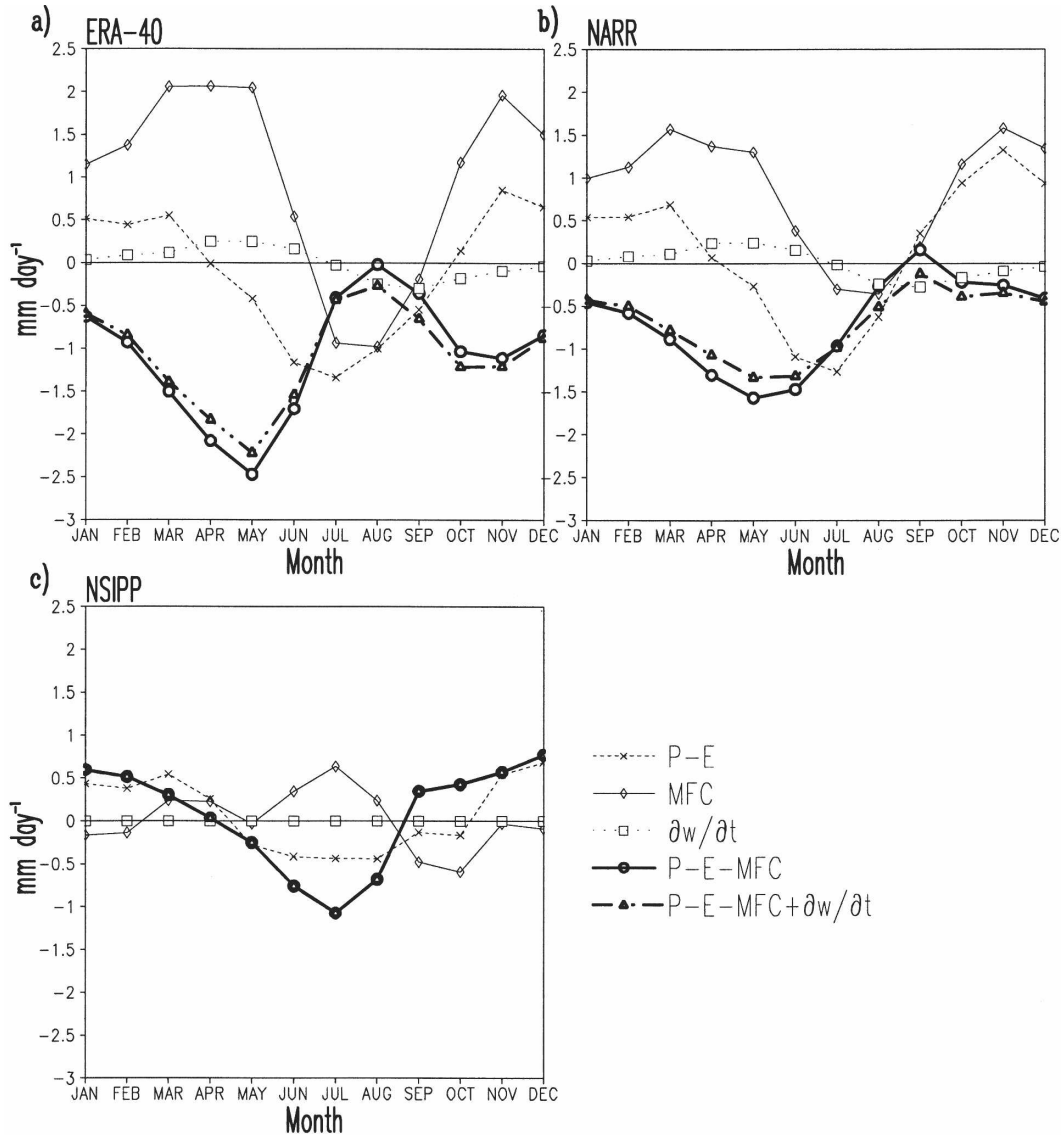


FIG. 14. Atmospheric water balance over the Great Plains (climatology) in mm day^{-1} : (a) ERA-40 reanalysis, (b) NARR reanalysis, and (c) NSIPP simulation. $P - E$: short dashed line with Xs; MFC: thin continuous line with diamonds; $\partial W/\partial t$: dotted line with squares; $P - E - MFC$: thick continuous line with circles; and $P - E - MFC + \partial W/\partial t$: thick dot-dot-dash line with triangles.

- Station and satellite-based precipitation differences pale in comparison with the departures of global reanalyses from observations: the eastern United States is drier in ERA-40 and wetter in NCEP, by up to a third in each case. The annual means, in fact, mask even larger but offsetting departures of winter and summer precipitation, especially, over the southeastern United States.
- ERA-40 exhibits more reasonable seasonal variability of precipitation. NCEP has excessive annual-cycle amplitude across the United States, particularly over the southeast, where observed amplitudes are negli-

gible. Broadly speaking, CAM3.0 is like ERA-40, while NSIPP is closer to NCEP reanalysis. The rainy season over the Great Plains and northern tier states peaks a month earlier in NCEP data.

- Land-ocean competition for convection is too intense in the models (and even NCEP reanalysis), so much so that the oceanic ITCZ in July (Mexican monsoon's peak phase) is southward of its winter position in both simulations—not to mention, the intense Mexican monsoon in simulations and NCEP reanalysis. The possibility that the ITCZ location error arises from overconstrained model simulations

(globally specified SST and sea ice boundary conditions) was ruled out by examination of NCAR's coupled model (CCSM3) simulation, which was found to be similarly afflicted.

- Overresponsiveness of land is also manifest in the models' surface air temperature; the winter-to-summer change over Great Plains is 5–9 K larger than in observations, with implications for modeling of climate sensitivity, since CAM3.0 is used in IPCC assessment, as a component of NCAR's CCSM3.0 climate system model.
- Summer sea level pressure anticyclones—Pacific high and the Bermuda high—exert opposite influences on the adjoining coasts. The former suppresses summer precipitation on the west coast from dynamically induced subsidence over its eastern arm, while the latter encourages it on the eastern seaboard by inducing convergence over its western arm. Both influences are reasonably represented in the reanalyses and model simulations.
- The anticyclonic circulation reaching the continental interior in summer—comprising easterly flow over the Caribbean and a southerly jet leaning against eastern slopes of the Sierra Madre Oriental range—is well represented in all reanalyses. Summer flux convergence over the U.S. Gulf Coast and Great Plains however differs considerably between global and regional reanalyses. Models capture the essence of the circulation, but the features are more diffuse.
- Winter moisture fluxes are more consistently represented in reanalyses and model simulations because atmosphere–land surface interactions are relatively muted in this season.
- Choice of rainy season in the Pacific Northwest is influenced by stationary moisture flux *convergence*, which, unlike transient convergence, is seasonally sensitive. Dynamically induced convergence (and ascent) along the eastern flank of the Aleutian low is influential in winter being the rainy season, that is, vorticity balance considerations (and induced vertical motions) rather than moisture transport ones are determining. More analysis is clearly needed.
- Reanalysis evaporation is larger than the offline-produced estimates, except in autumn; summer values are larger by a factor of up to 2. Model evaporation is somewhere in between and cannot be considered excessive. Interestingly, these very models produce very large evaporation *anomalies* over the Great Plains in context of interannual variability; anomalies larger than both offline and reanalysis based estimates, by a factor of up to 4 (RBN).
- Examination of atmospheric water *cycle* over the

Great Plains shows precipitation evolution to be realistic in winter and early spring, but not autumn, when global reanalyses and models underestimate precipitation by a factor of up to 2. Total moisture flux convergence evolves consistently in reanalyses but with varying amplitude: strongest in ERA-40 and weakest in NARR, but significant in both cases, especially during October–March when convergent fluxes are the primary source of moisture. Evaporation picks up notably in April and remains the leading contributor until September.

- Investigation of atmospheric water *balance* over the Great Plains reveals substantially unbalanced moisture budgets in both reanalysis and simulations. Imbalance in NARR is smaller than ERA-40's, but unacceptably large, nonetheless. The imbalance is most pronounced in spring and summer, and must result from excessive evaporation in this period.

Despite successful assimilation of precipitation in NARR, its diagnosis of evaporation remains suspect—in part because evaporation (or soil moisture) is not *directly* nudged during the assimilation process. NARR's present assimilation strategy focuses on thermodynamics of the atmospheric column, paying no regard to dynamics (circulation and fluxes) and the underlying land surface (e.g., soil moisture). Adjusting the latter can lead to more balanced regional atmospheric water budgets and help realize NARR's goal of generating realistic regional-to-continental-scale hydroclimate fields over North America.

An unbalanced atmospheric water budget must have footprints in the land surface energy balance. An examination of the spatiotemporal structure of radiative fluxes and Bowen's ratio is currently underway to better understand the origin of seasonal atmospheric water imbalance over the Great Plains.

The present study underscores the need to develop innovative reanalysis strategies—ones constrained by minimization of water and energy imbalances, in addition to canonical short-term forecast error reduction. Only then will retrospective analyses be useful for climate studies. Development of climate data assimilation will thus require a change of mind-set, but it is within the means and ability of our science to deliver.

Acknowledgments. The authors would like to acknowledge support of Grants DOE-CCPP DEFG 0201ER63258, NASA-NSIPP NAG512417, and NSF ATM-0445136. Sumant Nigam would like to thank Suki Manabe for helpful discussions and encouragement. The authors thank David Straus (Editor) and two reviewers for their constructive input.

REFERENCES

- Boyle, J. S., 1998: Evaluation of the annual cycle of precipitation over the United States in GCMs: AMIP simulations. *J. Climate*, **11**, 1041–1055.
- Dirmeyer, P. A., and L. Tan, 2001: A multi-decadal global land-surface data set of state variables and fluxes. COLA Tech. Rep. 102, 43 pp. [Available from the Center for Ocean–Land–Atmosphere Studies, 4041 Powder Mill Road, #302, Calverton, MD 20705.]
- Ek, M. B., K. E. Mitchell, Y. Lin, E. Rogers, P. Grunmann, V. Koren, G. Gayno, and J. D. Tarpley, 2003: Implementation of Noah land surface model advances in the National Centers for Environmental Prediction operational meso-scale Eta model. *J. Geophys. Res.*, **108**, 8851, doi:10.1029/2002JD003296.
- Gates, W. L., and Coauthors, 1999: An overview of the results of the Atmospheric Model Intercomparison Project (AMIP I). *Bull. Amer. Meteor. Soc.*, **80**, 29–56.
- Higgins, R. W., K. C. Mo, and S. D. Schubert, 1996: The moisture budget of the central United States in spring as evaluated from the NCEP/NCAR and the NASA/DAO reanalyses. *Mon. Wea. Rev.*, **124**, 939–963.
- , Y. Yao, E. S. Yarosh, J. E. Janowiak, and K. C. Mo, 1997: Influence of the Great Plains low-level jet on summertime precipitation and moisture transport over the central United States. *J. Climate*, **10**, 481–507.
- Hoskins, B. J., 1996: On the existence and strength of the summer subtropical anticyclones. *Bull. Amer. Meteor. Soc.*, **77**, 1287–1291.
- Hsu, C.-P. F., and J. M. Wallace, 1976: The global distribution of the annual and semiannual cycles in precipitation. *Mon. Wea. Rev.*, **104**, 1093–1101.
- Huang, J., H. M. Van den Dool, and K. P. Georgarakos, 1996: Analysis of model-calculated soil moisture over the United States (1931–1993) and applications to long-range temperature forecasts. *J. Climate*, **9**, 1350–1362.
- Jones, P. D., and A. Moberg, 2003: Hemispheric and large-scale surface air temperature variations: An extensive revision and an update to 2001. *J. Climate*, **16**, 206–223.
- Kalnay, E., and Coauthors, 1996: The NCEP/NCAR 40-Year Reanalysis Project. *Bull. Amer. Meteor. Soc.*, **77**, 437–471.
- Lindzen, R. S., and S. Nigam, 1987: On the role of sea surface temperature gradients in forcing low-level winds and convergence in the Tropics. *J. Atmos. Sci.*, **44**, 2418–2436.
- Mesinger, F., and Coauthors, 2004: NCEP North American regional reanalysis. Preprints, *15th Symp. on Global Change and Climate Variations*, Seattle, WA, Amer. Meteor. Soc., CD-ROM, P1.1.
- Mitchell, K., and Coauthors, 2004: NCEP completes 25-year North American Reanalysis: Precipitation assimilation and land surface are two hallmarks. *GEWEX Newsletter*, No. 14, International GEWEX Project Office, 9–12.
- Mitchell, T. P., and J. M. Wallace, 1992: The annual cycle in equatorial convection and sea surface temperature. *J. Climate*, **5**, 1140–1156.
- Mo, K. C., and R. W. Higgins, 1996: Large-scale atmospheric moisture transport as evaluated in the NCEP/NCAR and the NASA/DAO reanalyses. *J. Climate*, **9**, 1531–1545.
- Nigam, S., and Y. Chao, 1996: Evolution dynamics of tropical ocean–atmosphere annual cycle variability. *J. Climate*, **9**, 3187–3205.
- Rasmusson, E. M., 1967: Atmospheric water vapor transport and the water balance of North America: Part I. Characteristics of the water vapor flux field. *Mon. Wea. Rev.*, **95**, 403–426.
- , 1968: Atmospheric water vapor transport and the water balance of North America: Part II. Large-scale water balance investigations. *Mon. Wea. Rev.*, **96**, 720–734.
- , and K. C. Mo, 1996: Large-scale atmospheric moisture cycling as evaluated from NMC global analysis and forecast products. *J. Climate*, **9**, 3276–3297.
- Rayner, N. A., D. E. Parker, E. B. Horton, C. K. Folland, L. V. Alexander, D. P. Rowell, E. C. Kent, and A. Kaplan, 2003: Globally complete analyses of sea surface temperature, sea ice and night marine air temperature, 1871–2000. *J. Geophys. Res.*, **108**, 4407, doi:10.1029/2002JD002670.
- Roads, J. O., S.-C. Chen, A. K. Guetter, and K. P. Georgarakos, 1994: Large-scale aspects of the United States hydrologic cycle. *Bull. Amer. Meteor. Soc.*, **75**, 1589–1610.
- Ropelewski, C. F., and E. S. Yarosh, 1998: The observed mean annual cycle of moisture budgets over the central United States. *J. Climate*, **11**, 2180–2190.
- Ruiz-Barradas, A., and S. Nigam, 2005: Warm-season rainfall variability over the U.S. Great Plains in observations, NCEP, and ERA-40 reanalyses, and NCAR and NASA atmospheric model simulations. *J. Climate*, **18**, 1808–1830.
- Starr, V. P., and J. P. Peixoto, 1958: On the global balance of water vapor and the hydrology of deserts. *Tellus*, **10**, 189–194.
- Trenberth, K. E., and C. J. Guillemot, 1998: Evaluation of the atmospheric moisture and hydrological cycle in the NCEP/NCAR reanalyses. *Climate Dyn.*, **14**, 213–231.
- Xie, P., and P. Arkin, 1996: Analyses of global monthly precipitation using gauge observations, satellite estimates, and numerical model predictions. *J. Climate*, **9**, 840–858.

Copyright of *Journal of Climate* is the property of *American Meteorological Society* and its content may not be copied or emailed to multiple sites or posted to a listserv without the copyright holder's express written permission. However, users may print, download, or email articles for individual use.